https://doi.org/10.5194/essd-2025-260
Preprint. Discussion started: 28 May 2025

Open Access Earth System Science Data Discussions

Geospatial micro-estimates of slum populations in 129 Global South countries using machine learning and public data

Dan Li[a], Laixiang Sun[b,c,*], Yang Yu[d], Peipei Tian[a]

[a] Institute of Blue and Green Development, Shandong University, Weihai, 264209, China
[b] Department of Geographical Sciences, University of Maryland, College Park, 20742, MD, USA
[c] School of Finance & Management, SOAS University of London, London, WC1H 0XG, UK
[d] Division of Liberal Studies, Howard Community College, Columbia, MD 21044, United States.

* Corresponding author: lsun123@umd.edu (L.S.)

https://doi.org/10.5194/essd-2025-260
Preprint. Discussion started: 28 May 2025

Abstract

Slums are a visible manifestation of poverty in Global South countries. Reliable estimation of slum population is crucial for urban planning, humanitarian aid provision, and improving well-being. However, large-scale and fine-grained mapping is still lacking due to inconsistent methodologies and definitions across countries. Existing datasets often rely on government statistics, lacking spatial continuity or underestimating slum population due to factors such as city image and privacy concerns. Here, we develop a standardized bottom-up approach to estimate slum population at the neighborhood level (~6.72 km resolution at the equator) for 129 Global South countries in 2018. Leveraging the Sustainable Development Goals 11.1 framework and machine learning, our estimation integrates household-based surveys, satellite imagery, and grided population data. Our models explain 82% to 96% of the variation in ground-truth surveys, with a root mean squared error of 4.85% to 10.47%, outperforming previous benchmarks. Cross-validation with independent data confirms the reliability of our estimates. To our knowledge, this is the first comprehensive geospatial inventory of slum populations across Global South countries, offering valuable insights for advancing urban sustainability and supporting further research on vulnerable populations. The maps of slum populations and their local shares in Global South countries are available in the Zalando repository at https://doi.org/10.5281/zenodo.13779003 (Li et al., 2025).

Introduction

The right to adequate housing and shelter holds a central position in the realm of international human rights (Hohmann, 2013; Nowak, 2021). However, a distressing reality persists: millions of individuals worldwide live in life- or health-threatening conditions, commonly referred to as slums, informal settlements, favelas, or shanties (Hardoy et al., 2013). As a kind of visible expressions of poverty, slums are typically characterized by physical state of disrepair, degraded environment in insanitary conditions, and absence of basic and essential facilities, and they are often situated in disadvantageous, exposed and hazardous areas (Abascal et al., 2022; UN-Habitat, 2004). The emergence and persistence of slums have been a consequence of rapid and unplanned urbanization that outpaces economic growth and infrastructure development (Ezeh et al., 2017; Marx et al., 2013). According to the World Cities Report 2020 (UN-HABITAT, 2020), over 1 billion people live in urban slums, with 80% of them residing in cities within developing countries. Nevertheless, urbanization has not yet peaked, and the population living in slum-like conditions is expected to grow (Guan et al., 2018; UN-HABITAT, 2020). This intensifies the urgency to provide adequate housing, basic services and slums upgrades, in line with the commitment to the Sustainable development Goals (SDG) and "leaving no one behind" (Weber, 2018; Tian et al., 2024).

Reliable slum population estimates are essential for understanding the spatial scale and distribution of slum populations, providing foundational data for implementing targeted urban planning and improving human well-being (Parikh et al., 2013; Satterthwaite et al., 2020; Schetke et al., 2012). These estimates help identify vulnerable populations, similar to demographic data on the elderly and women (Singh, 2016). Detailed knowledge of slum population locations enables effective resources allocation and targeted interventions (Doe et al., 2020; Zhou et al., 2022). Quantitative data can also motivate policymakers and researchers to tackle inequalities, while spatial knowledge can help pinpoint drivers of slum population growth, such as proximity to rivers and elevation, thus contributing to climate risk management (Baynes et al., 2022; Rentschler et al., 2023; Sietchiping and Yoon, 2010).

Despite this, large-scale, comparable inventories of slum populations remain scarce. National statistics and sparce survey data, such as those from censuses or Know Your City Campaigns, fail to provide a spatially continuous view of slum population (Angeles et al., 2009; Pedro and Queiroz, 2019; Persello and Kuffer, 2020). These data collections are inconsistent across countries (Thomson et al., 2020), and governments may withhold or omit sensitive information due to factors such as city image considerations (Björkman, 2013; Moreno, 2003; Wurm et al., 2017). Privacy concerns also contribute to underreporting (Engin et al., 2020), as slum dwellers may distrust external inquiries (Binzel and Fehr, 2013; Rogler, 1967). As a result, spatially explicit data on slum populations, particularly in developing countries, remain scarce.

Recent advancements in machine learning and the availability of satellite imagery provide new opportunities for slum population mapping (Burke et al., 2021; Gram-Hansen et al., 2019; Wurm et al., 2019). While considerable research has focused on identifying slums based on satellite-derived morphological features, such as studies in Mumbai (Ibrahim et al., 2019), and Kenya (Mahabir et al., 2020), these efforts are often limited to individual cities (Banerjee et al., 2017;

Thomson et al., 2020) and may not provide comparable results across countries or regions. For instance, the boundaries of slum determined in these studies may yield discrete outcomes (Patel et al., 2019), making it difficult to integrate this information with population data to produce large-scale demographic insights (Breuer and Friesen, 2023). In some cases, there might be a necessity to obfuscate the precise boundaries of slums to safeguard the privacy of already vulnerable populations (Thomson et al., 2019). Although several studies have estimated slum populations in selected cities across the Global South, these estimates are generally considered to be underestimations (Breuer et al., 2024; Thomson et al., 2022).

In this study, we integrate ground-surveys, public satellite imagery, and advanced machine learning to map slum population at the cluster-level (6.72km × 6.72km at the equator) across Global South countries. During the training, validation, and testing phases, we assemble data from surveys covering over 1 million households in 67,204 clusters across 53 countries, sourced from Demographic and Health Surveys (DHS). Using this data, we construct a slum indicator framework and fine-tune the ResNet-34 algorithm to extract features from Landsat and nighttime light imagery. For out-of-sample predictions, we apply the cross-validated model to predict slum indicators and integrate them with grided population data to create detailed slum population maps for 129 Global South countries in 2018. Overall, we offer a generalized and scalable approach to slum population mapping that enables regional comparisons while maintaining privacy safeguards. The objectives of this study are to (1) develop a machine learning-based workflow for slum population mapping, (2) generate a fine-grained inventory of slum population in 129 Global South countries, and (3) analyze spatial distribution disparities across different geographic regions and income groups.

2 Dataset description

Four types of publicly accessible datasets are used in this study. The first type is geo-referenced household surveys, which are used to calculate the slum indicator as machine learning labels. The second type consists of daytime satellite imagery and nighttime light imagery, which serve as the input features. The third type is grided population data, used in combination with the slum indicator to produce the final gridded slum population estimates. The fourth type consists of gridded auxiliary data related to slum populations, which help exclude areas

https://doi.org/10.5194/essd-2025-260
Preprint. Discussion started: 28 May 2025

without human settlements. Table 1 outlines the datasets and layers that are used to generate the slum population map in this study.

Table 1. Overview of data sources for generating the slum population map in Global South countries

Data Sources	Abbreviation	Input spatial resolution	Period Coverage	Reference
Demographic and Health Survey	DHS (https://www.dhsprogram.com/Data/)	household-based data, ~2km for urban areas and ~5km sometimes 10km for rural areas	The latest version for 53 countries varying from 2010~2020	Rutstein and Staveteig (2014)
Landsat Collection 2 on Google Earth Engine	Landsat 8 Level 2, Collection 2, Tier 1 (https://developers.google.com/earth-engine/datasets/catalog/LANDSAT_LC08_C02_T1_L2) Landsat 7 Level 2, Collection 2, Tier 1 (https://developers.google.com/earth-engine/datasets/catalog/LANDSAT_LE07_C02_T1_L2)	30m	Landsat 7 ETM+: 1999~2024 Landsat 8 OLI/TIRS: 2013~2024	Tamiminia et al. (2020); Roy et al. (2016)
Global NPP-VIIRS-like nighttime light data (through a new cross-sensor calibration from DMSP-OLS NTL data and a composition of monthly NPP-VIIRS NTL data.	An extended time-series (2000-2023) of global NPP-VIIRS-like nighttime light data (https://doi.org/10.7910/DVN/YGIVCD)	15 arcsec (~500 m)	2000~2023	Chen et al. (2020); Elvidge et al. (2017); Hsu et al. (2015)
Global Human Settlement Population Grid	GHS-POP (https://human-settlement.emergency.copernicus.eu/download.php?ds=pop)	1km	2020	Schiavina et al. (2022)
Global Human Settlement Model Grid	GHS-SMOD (https://human-settlement.emergency.copernicus.eu/download.php?ds=smod)	1km	2020	Schiavina et al. (2022)
Copernicus	Copernicus Global Land Cover Layers: CGLS-LC100 Collection 3 (https://developers.google.com/earth-engine/datasets/catalog/COPERNICUS_Landcover_100m_Proba-V-C3_Global)	100m	2018	Buchhorn et al. (2020)

2.1 Geo-referenced household surveys

This study uses the household-based ground survey data from Demographic and Health Surveys (DHS) to calculate the proportion of slum households at the cluster-level. The DHS program is funded primarily by the United States Agency for International Development (USAID), and collects nationally representative and comparable information based on a consistent set of questionnaires for a wide range of monitoring and impact evaluation indicators in the areas of population, health, and household living conditions in developing countries (Rutstein and Staveteig, 2014). The derived standard DHS Surveys have large sample sizes (usually between 5,000 and 30,000 households) and typically are conducted

https://doi.org/10.5194/essd-2025-260
Preprint. Discussion started: 28 May 2025

about every 5 years. Focusing on Global South countries, we deprive the geo-referenced data from 53 countries (as of 2022) in Latin American, Africa and Asia, with a valid dataset comprising over 1 million households across 67,204 clusters. The ground-truth household surveys points can be found in Figure S1 and Table S1. To protect respondent confidentiality, the DHS program randomly displaces the geographic coordinates of the surveyed locations, with a maximum of 2km for urban clusters and 5km or sometimes 10 km for rural clusters (Burgert et al., 2013). To avoid misclassification in analysis using administrative-level data, the displacements are constrained within the administrative boundaries, specifically at the administrative level 3 (Figure S2). The cluster level thus corresponds to neighborhoods in urban areas or villages in rural areas.

2.2 Satellite imagery

We collect publicly available Landsat-7 ETM+ (Collection 2, Tier 1), Landsat-8 OLI (Collection 2, Tier 1) and nighttime light imagery centered on each cluster from Google Earth Engine platform (Tamiminia et al., 2020) and Global NPP-VIIRS-like nighttime light dataset (Chen et al., 2020). Landsat imagery series offer the world's longest-running collection of consistently acquired, high-resolution earth observation data, and have been applied in numerous studies such as urban growth monitoring. The collection 2, Tier 1 images have undergone improved systematic geometric correction and radiometric calibration. Due to differences in the spectral reflectance between different sensors, we adopt the normalization coefficients from Roy et al. (2016) to characterize the ETM+ reflectance to that of OLI. To get clear slices with fewer clouds and snow, we generate a 1-year median composite from Landsat imagery by selecting cloud-free pixels based on the quality assessment (QA) bands, and then calculating the median value for each available cloud-free pixel over the 1-year period (Azzari and Lobell, 2017). Similarly, considering the inconsistent timing of household surveys across countries, we use the Global NPP-VIIRS-like nighttime light dataset to ensure spatiotemporal consistency between satellite imagery and slum indicator labels. This NPP-VIIRS-like dataset, produced through cross-sensor calibration of the DMSP-OLS and NPP-VIIRS datasets, is particularly suitable for analyzing long-term demographic and socioeconomic trends. We thus obtain six multispectral bands from Landsat imagery including red, green, blue, near infrared and two

https://doi.org/10.5194/essd-2025-260
Preprint. Discussion started: 28 May 2025

Open Access Earth System Science Data Discussions

shortwave infrared bands, and one single band from NPP-VIIRS-like nighttime light dataset. The Landsat and Nighttime light slices have a size of 224 × 224 tiles, in accordance with the input size of our convolutional neural networks architecture and covering the extent of displacement. Consequently, our mapping resolution is determined to be 6.72 kilometers on equator (30m-pixel size × 224 pixels = 6.72 km).

2.3 Population and gridded auxiliary data

We utilize and process the 1km-gridded Global Human Settlement Population dataset (GHS-POP), developed by the EU Joint Research Center, to estimate the slum population (Schiavina et al., 2022). The GHS-POP dataset provides a more precise estimation of population distribution by disaggregating census or administrative unites into grid cells, based on the classification of built-up areas in the Global Human Settlement Layer derived from Landsat imagery. It is selected for its superior accuracy and top-down constrained allocation approach, outperforming other available gridded population datasets (Smith et al., 2019; Tellman et al., 2021). We resample this population dataset to match the resolution of our cluster level mapping. Additionally, we incorporate the GHS Settlement Model Grid (GHS-SMOD) and the Copernicus Global Land Cover Layers product (CGLS-LC100) as auxiliary grided data (Buchhorn et al., 2020; Schiavina et al., 2022). This helps us differentiate settlement patterns across urban, semi-urban, and rural areas, and also allows us to exclude areas with low population density.

3 Methodology

We propose a standardized and comparable framework for estimating cluster-level slum population, which integrates a slum indicator framework based on the definition of slum households, a deep learning model, and an XGBoost ensemble classifier. Our approach addresses the underestimation of slum population in prior literature, which heavily relied on slum boundary geometry. A set of examples of the uncertainties in slum boundary delineation is shown in Figure S3. Figure 1 depicts the flowchart for mapping slum populations in Global South countries. The main procedures are outlined as follows.

https://doi.org/10.5194/essd-2025-260
Preprint. Discussion started: 28 May 2025

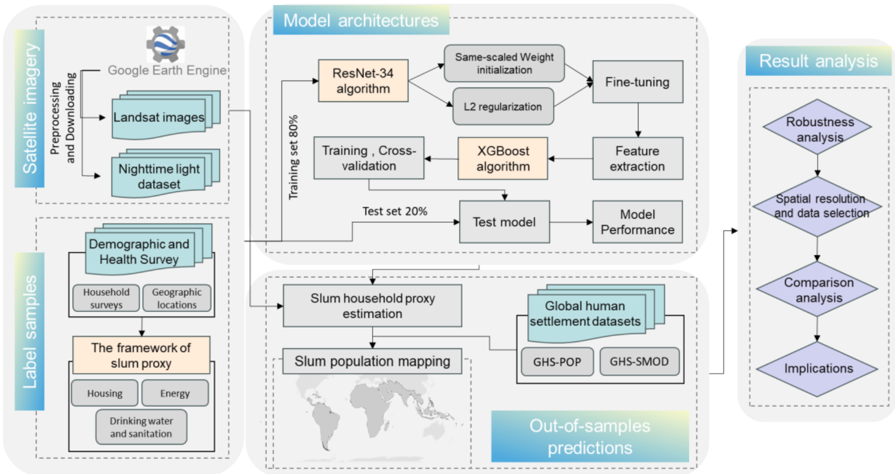

Figure 1 Flowchart of this study

3.1 Framework of slum indicator

We use the SDG 11.1 framework as a proxy to estimate the occurrence of households living in slums or slum-like conditions within a cluster. Based on UN-Habitat's definition of a slum household (UN-habitat, 2021), we incorporate "access to electricity" into our slum population framework, recognizing its critical role in human well-beings in developing countries. However, we exclude the "security of tenure" dimension due to data limitations. As a result, the slum population is defined as individuals (or households) living in conditions lacking one or more of the following: safely and adequate housing, safely managed drinking water and sanitation services, or reliable and modern energy services. These conditions are categorized into three dimensions, comprising ten indicators (Table 2). The specific definitions and criteria are detailed in Table S2. We treat housing, water and sanitation, and electricity as equally important, assigning each a weight of 0.33. The slum indicator is then determined as follows:

$$S_c = \frac{1}{NH_c} \cdot \left(w_H \cdot \frac{\sum_{i=1}^{n_H} h_{i,c}}{n_H} + w_W \cdot \frac{\sum_{j=1}^{n_W} wa_{j,c}}{n_W} + w_E \cdot \frac{\sum_{l=1}^{n_E} e_{l,c}}{n_E}\right) \cdot 100\% \qquad (1)$$

where S_c represents the slum indicator for each cluster c; NH_c is the total number of households in cluster c; w_H, w_W, and w_E represent the weights assigned to the dimensions of safely and adequate housing (H), safely managed drinking water and sanitation services (W), and reliable and modern energy services (E); n_H, n_W,

https://doi.org/10.5194/essd-2025-260
Preprint. Discussion started: 28 May 2025

n_E represent the total number of sub-indicators within the H, W and E dimensions, respectively; $h_{i,c}$, $wa_{j,c}$, and $e_{l,c}$ denote the numbers of households in cluster c that fail to meet the criteria for the i-th housing sub-indicator, j-th water and sanitation sub-indicator, and l-th energy sub-indicator, respectively.

Table 2 The framework of slum indicator based on household data

Dimensions	Indicators
Safely and adequate housing	House made of finished materials (roof, wall and floor)
	House with a sufficient living room
Safely managed drinking water and sanitation services	Household using safely managed drinking water
	Household with access to water availability for continuous two weeks
	Household with access to drinking water located within a round trip of 30 minutes
	Household using safely managed sanitation toilets
	Household using safely managed hand-washing facility with water.
	Household using safely managed hand-washing facility with soap or detergent
Reliable and modern energy services	Household with access to electricity
	Household with clean cooking fuels

3.2 Model architecture

We employ transfer learning by fine-tuning the pre-trained ResNet-34 to extract the informative features from satellite imagery (Figure 2). Transfer learning in deep learning leverages pre-trained models, which have been trained on large datasets, to capture general features with high accuracy (Pan and Yang., 2009). In this study, we start with a ResNet model pre-trained on the large ImageNet dataset, which comprises over 100 million samples. ResNet, standing for the Residual Network, is a deep convolutional neural network (CNN) architecture that uses skip connections to bypass one or more layers, allowing input data to be added directly to the output (He et al., 2016). These skip connections help mitigate the vanishing or exploding gradient problems often encountered in deep networks. ResNet-34 strikes a balance between model depth

https://doi.org/10.5194/essd-2025-260
Preprint. Discussion started: 28 May 2025

and computational efficiency, making it an idea choice for fine-grained mapping tasks (Robinson et al., 2017; Shi et al., 2022) while offering a good trade-off between model capacity and accuracy (Russakovsky et al., 2015).

For the purpose of this study, we modify the first convolutional layer to accommodate our satellite slice inputs, and the last layer to produce a continuous estimate instead of a classification. Specifically, we initialize the RGB channels with weights pre-trained on ImageNet, while for non-RGB channels, we use the average of weights for RGB weights for initialization, scaling all weights by 3/7. Following Yeh et al., (2020), the remaining layers of the ResNet are initialized to their ImageNet values, and the weights for the final layer are initialized randomly. The model is trained using Adam optimizer (Kingma and Ba, 2014) and a mean squared-error loss function with L_2 regularization. The models are trained for 120 epochs, with early stopping implemented to prevent overfitting. The hyperparameter learning rate and L_2 weight regularization are ranged among 0.1, 0.01, 0.001 and 0.0001, and 1, 0.1, 0.01 and 0.001, respectively. After fine-tuning the ResNet-34 model, we leverage it to extract 512-dimensional features from the satellite images. Here we do not incorporate other slum-related geographical characteristics, such as proximity to government agencies or educational facilities, since these quantifications are not sufficiently accurate due to the displacement of cluster locations as indicated in DHS documentations.

Subsequently, we use eXtreme Gradient Boosting tree (XGBoost), a popular and flexible supervised-learning algorithm, to predict the occurrence of slum household in each cluster from 512 features. XGBoost, introduced by Chen and Guestrin (2016), is a scalable machine learning model based on the gradient boosting framework. It builds an ensemble of decision trees by sequentially adding weak learners, each aimed at improving prediction accuracy. The first tree is constructed by splitting features to minimize the loss function, and subsequent trees are generated iteratively, correcting the residuals of previous predictions. This process continues until the stopping criteria are met. In XGBoost, the trees work together to progressively reduce residuals, with the final prediction obtained by aggregating the outputs of all trees. XGBoost is renowned for its high speed and strong predictive performance, particularly well-suited for large datasets and high-dimensional data.

https://doi.org/10.5194/essd-2025-260
Preprint. Discussion started: 28 May 2025

Open Access Earth System Science Data Discussions

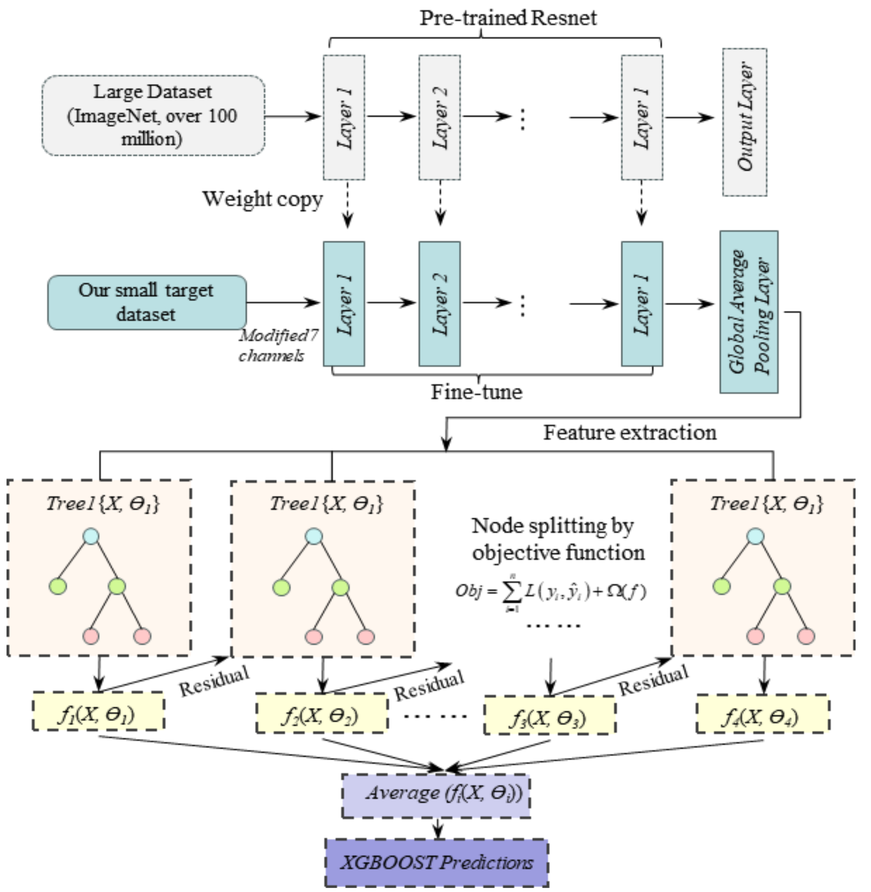

Figure 2 The model architecture for integrating transfer learning using ResNet-34 as the feature extractor and XGBoost for regression.

We perform a grid search to find the optimal combinations of hyperparameters and apply L_2 regularization to the loss function to prevent overfitting. The hyperparameters tuned include the learning rate (learning_rate), the maximum depth of trees (max_depth), the fraction of the training data used for building each tree (subsample), the fraction of features used for each tree (colsample_bytree), the regularization term to control tree complexity (gamma), and the total number of boosting rounds (n_estimators). By optimizing these parameters, we ensure the model achieves a balance between predictive performance and generalization. These optimal hyperparameters are then applied

https://doi.org/10.5194/essd-2025-260
Preprint. Discussion started: 28 May 2025

to retrain the model on the entire dataset, producing the final model for out-of-sample estimation. Table 3 lists the candidate values considered during the grid search.

Table 3 The hyperparameters used in grid search

Hyperparameters	Param_grid
learning_rate	[0.01, 0.03, 0.05, 0.1]
max_depth	[3, 5, 6, 7]
subsample	[0.6, 0.8, 1.0]
colsample_bytree	[0.6, 0.8, 1.0]
gamma	[0, 0.1, 0.2, 0.3]
n_estimators	[best_num_boost_rounds]

3.3 Model training and cross validation

During the model training and cross validation phases, we divide the 53 countries with the DHS data into 9 groups based on their geographical regions and income levels (Table S3). In other words, we train nine separate regional models, following the flowchart in Figure 1. To enhance the generalization ability of the models, we group countries for training and validation rather than training individual country-specific models, ensuring a sufficient number of samples per group. While our primary focus is on regional models, we also compare their performance against country-specific models to evaluate potential differences.

We split the spatial-temporal matched satellite images and DHS survey labels into training, validation, and test sets. Specifically, 20% of the dataset is held out as an independent test set to assess the final model's performance, while the remaining 80% is used for training and validation. For robust model evaluation, we employ 5-fold spatially stratified cross-validation. In each fold, the data is divided to maintain equal proportions of urban and rural samples, as well as consistent proportions of samples from each country within the group. During cross-validation, the model is trained on four folds and validated on the remaining fold, repeating the process five times so each fold serves as the validation set once. This rigorous approach enables accurate assessment of the model's generalization ability across different geographic regions and income levels, while ensuring an unbiased evaluation on the held-out test set.

https://doi.org/10.5194/essd-2025-260
Preprint. Discussion started: 28 May 2025

3.4 Out-of-samples predictions

Using our final models, we apply satellite imagery and nighttime light data to grid cells of 6.72-km in Global South countries, focusing on cells with populations exceeding 1,000. This allows us to estimate the cluster-level slum indicators across 129 Global south countries, based on the list of the United Nations' Finance Center for South-South Cooperation. Clusters with populations below 1000 are excluded to avoid unreliable out-of-sample estimates.

To produce the final map of population living in slums or slum-like conditions, we integrate the GHS-POP dataset with the map of cluster-level slum indicator. The slum indicator is used to clip the GHS-pop population grid, and to re-sample the population data for achieving spatial alignment. By combining the slum prevalence map with grided population dataset, we produce the final map of slum population at the cluster-level.

3.6 Evaluation approaches

Our slum population framework integrates multiple data sources, making robustness and uncertainty assessment complex. To address this, we adopt a step-by-step evaluation process, which involves validating results from intermediate steps and comparing results with other statistics (Haberl et al., 2021). We evaluate the performance of the final models using two metrics including coefficient of determination (R^2) and root mean squared error (RMSE). We cross-validate our mapped slum population estimates against a broad range of literature and statistical data at regional, national, and local scales. This comparison provides an additional layer of validation, helping to evaluate the consistency of our estimates with existing data.

To test the robustness of our framework, we evaluate the models under two alternative weighting schemes for the slum indicator: the “Basic Service” scenario and the “UN-Habitat” scenario. In the Basic Service scenario, greater emphasis is placed on water and sanitation, and energy services, with weights of 0.2, 0.4, and 0.4, respectively (Fu et al., 2019). In contrast, the UN-Habitat scenario prioritizes housing and water and sanitation services, assigning weights of 0.4, 0.4, and 0.2 (Mwaniki and Ndugwa, 2021). This sensitivity analysis helps determine how different weighting schemes affect the final predictions. We also compare the

https://doi.org/10.5194/essd-2025-260
Preprint. Discussion started: 28 May 2025

Open Access Earth System Science Data Discussions

performance of regional models with country-specific models to identify the strengths and limitations of applying a generalized model across different geographical areas.

4 Results

4.1 Model performance

To evaluate the performance of our regional models, we use two metrics, RMSE and R^2, to assess the predictive accuracy of the slum indicator at the cluster level in Africa, Asia, and Latin American regions, respectively (Table 4 and Figure 3). The optimal hyperparameters for the regional models are provided in Table S4. The household-based slum indicator calculated from DHS data serves as the ground truth, while our method generates the predicted values.

Overall, our regional models demonstrate strong performance, with RMSE values ranging from 5.20% to 10.17% and R^2 values between 0.82 and 0.95. Specifically, the models achieve an average RMSE of 5.89% in Africa, 6.66% in Asia, and 8.26% in Latin America. This performance may be attributed to the availability of labeled training data from household surveys used during the modeling process. When comparing performance across income groups, models developed for low-income and low-middle-income groups perform better than those for upper-middle-income and high-income groups in Asia and Latin America. It is worth noting that all models deliver satisfactory results.

In Figure 3, scatter points represent the distribution of true versus predicted values, and their even scatter around the 1:1 line indicates no significant overestimation or underestimation. Collectively, the results demonstrate the effectiveness of state-of-the-art machine learning models in capturing the complex relationships between satellite imagery and slum indicators. Given that local household survey data are not always available, our method offers a valuable approach for using limited data to identify the spatial distribution of slum households—a key indicator for estimating affordable and adequate housing, in alignment with SDG 11.1.

https://doi.org/10.5194/essd-2025-260
Preprint. Discussion started: 28 May 2025

Table 4 Model performance of slum indicator in Global South

Region	Income groups	Model	RMSE (%)	R^2
Africa	Low income	Model 1	5.29	0.93
		Model 2	5.88	0.89
	Lower middle income	Model 3	6.40	0.92
		Model 4	6.00	0.95
	Upper middle income	Model 5	8.92	0.83
Asia	Lower middle income	Model 6	5.20	0.84
	Lower middle income	Model 7	5.87	0.89
Latin American	Lower- middle and low income	Model 8	6.36	0.89
	High and upper middle income	Model 9	10.17	0.82

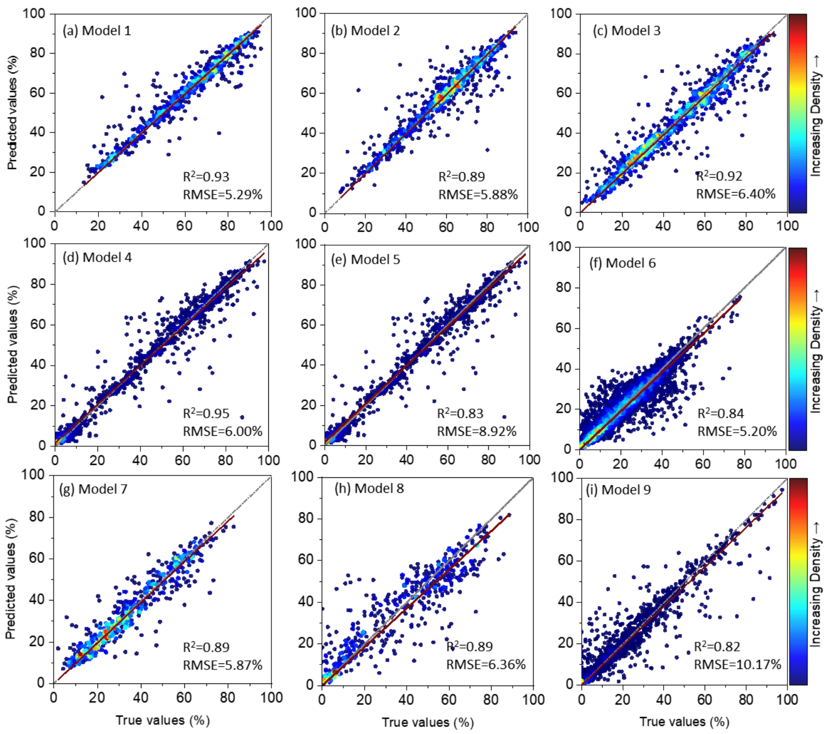

Figure 3 Model performances across different income groups. The true values represent the slum indicator calculated from DHS data using our slum framework, while the predicted values are produced by our machine learning-based models. For each model, a linear regression line is displayed alongside a reference line with a slope of one for comparison.

https://doi.org/10.5194/essd-2025-260
Preprint. Discussion started: 28 May 2025

4.2 Spatially explicit estimates of slum population in Global South

We apply the proposed framework to map slum population in 2018 across 129 Global South countries, including 54 in Africa, 42 in Asia and 33 in Latin America, using a spatial resolution of 3.63 arc-minutes (6.72 km on equator). The map is based on settlement slices, each having a population of over 1,000, and aligns with the delineations of urban and rural areas provided by the Global Human Settlement Layer. To refine the analysis, we also use the higher-resolution CGLS-LC100 dataset to mask out other land cover types from the settlement slices.

Figure 4a shows the spatial distribution of slum population across Global South countries. In terms of absolute numbers, slum population is concentrated in areas with expected high population densities, such as northern India in Asia, Rwanda and northern Morocco in Africa, and the coastal regions of Rio De Janeiro in Latin America, highlighted in dark blue on the map. Notably, more than 50% of the total slum population resides in less than 8% of the total grid cells.

Figure 4b highlights the administrative statistics and geographic disparities in slum population distribution. At the regional level, we estimate a total of over 0.88 billion people living in slums across the Global South. More than 60% of this population resides in South Asia and Sub-Saharan Africa, followed by East Asia and the Pacific (16%), the Middle East and North Africa (8.6%), Latin America and the Caribbean (7.4%), and Europe and Central Asia (1.7%).

When comparing urban slum populations to those living in slum-like conditions in rural areas, distinct urban-rural differences in settlement patterns emerge. In Latin America and the Caribbean, the Middle East and North Africa, Europe and Central Asia, and East Asia and the Pacific, a higher proportion of the slum population—between 46% and 60%—is concentrated in urban areas. In contrast, 41% of the slum population in South Asia is located in suburban areas, while 44% of those in Sub-Saharan Africa live in rural regions with slum-like conditions and inadequate services.

https://doi.org/10.5194/essd-2025-260
Preprint. Discussion started: 28 May 2025

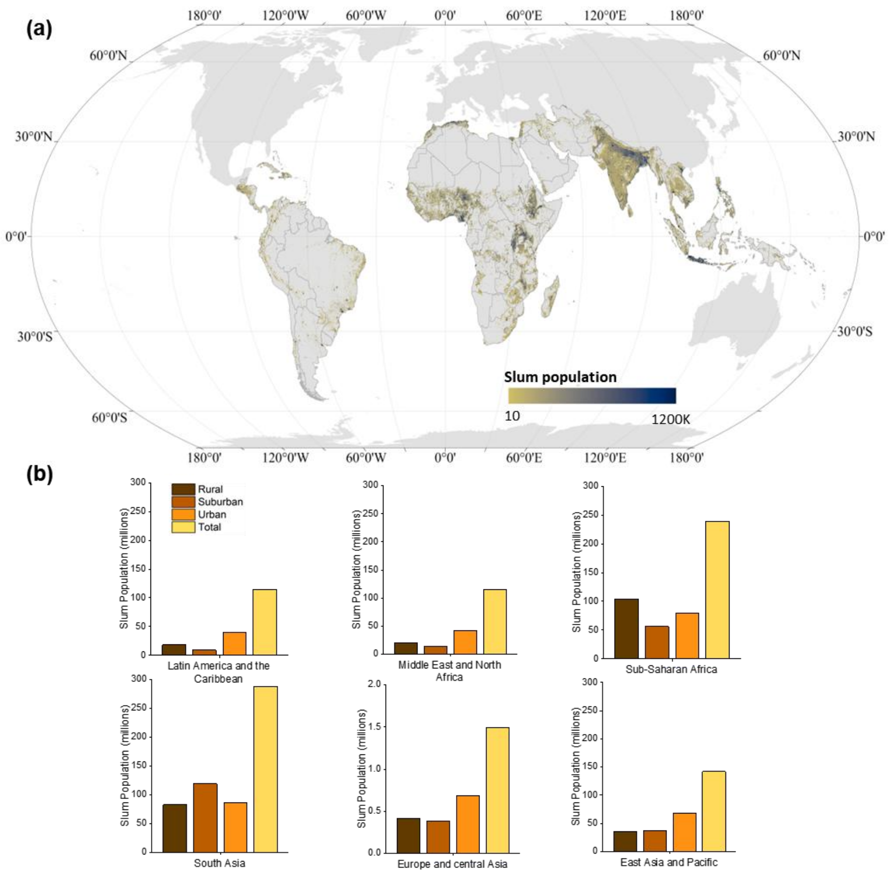

Figure 4 Spatial distribution of slum population in the Global South and their geographic disparities. (a) Map of slum population with a resolution of 3.63 arc-minutes. The settlement slices with a population of less than 1,000 are not included. (b) Statistics of slum population across geographic regions and disparities between rural and urban areas.

4.3 Mapping of local shares of slum population in Global South

We further estimate the local shares of slum population in Global South countries at a resolution of 3.63 arcminutes (Figure 5). These local shares allow for comparisons across countries and regions, accounting for differences in population sizes. Moreover, we implement a hierarchical classification of slum clusters, ranging from very low to very high concentrated levels, to reflect the extent to which local populations lack adequate infrastructure and housing within a community.

https://doi.org/10.5194/essd-2025-260
Preprint. Discussion started: 28 May 2025

As shown in Figure 5a, the spatial distribution of local shares provides new insights into the settlement pattern of slum population. For example, Sub-Saharan Africa exhibits notably high local shares of slum population, with 57% of the local population living in slum conditions. Within this region, countries like Libya and Nigeria show even higher local shares, reaching 70%. Comparatively, Latin America and Caribbean, South Asia, and East Asia have local slum population shares of 28%, 21% and 39%, respectively. Even in smaller countries such as Sierra Leone, the proportion of the population living in slums remains significant, at 60%.

We also analyze the concentration levels of slum clusters, from very low to very high, across income groups and regional groups (Figure 5b). Across the Global South, about 24% of the slum population resides in very highly concentrated slum clusters. In low-income countries, 60% of the slum population lives in clusters with very high concentration levels. In contrast, slum populations in high-income countries are less concentrated, with 45% living in moderately concentrated clusters. From a geographic perspective, Sub-Saharan Africa has the highest concentration, with 55% of the slum population living in very highly concentrated clusters. In other regions, slum populations are mainly concentrated at low or moderate levels.

The differing patterns of slum population concentration across Global South countries can be attributed to factors such as urbanization and uneven socioeconomic development. Our map provides rich spatial details on slum populations, both in terms of absolute numbers and local shares, making it a valuable tool for urban planning and slum upgrading initiatives.

https://doi.org/10.5194/essd-2025-260
Preprint. Discussion started: 28 May 2025

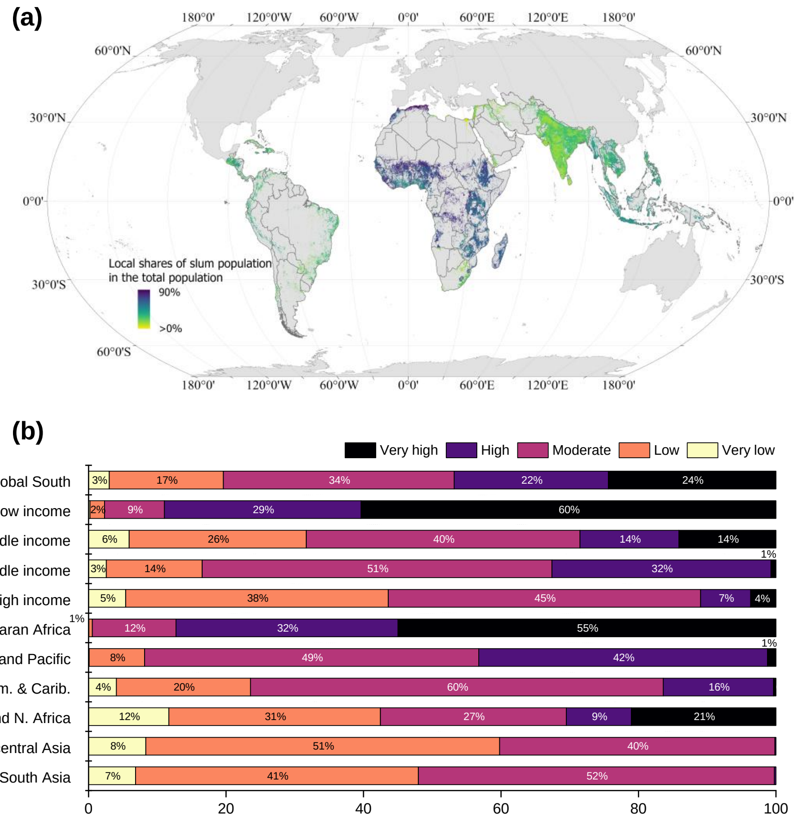

Figure 5 Slum populations categorized by concentration levels, ranging from very low to very high, and their geographic and socioeconomic disparities. (a) Map displaying local shares of the slum population at a resolution of 3.63 arcminutes. (b) Statistical analysis of disparities in slum population concentration across different regional and income groups. Concentration levels are classified based on the proportion of the slum population within each grid cell: very low (less than 10%), low (10%-20%), moderate (20%-40%), high (40%-60%) and very high (over 60%).

5 Discussions

We present a unified, scalable, and operational bottom-up approach for mapping slum populations. Our approach integrates location-specific data, state-of-the-art machine learning, satellite imagery, and population datasets. This approach enables slum population mapping over large areas and offers the

https://doi.org/10.5194/essd-2025-260
Preprint. Discussion started: 28 May 2025

Open Access Earth System Science Data Discussions

potential to predict slum populations with a high level of spatial detail in countries lacking survey-based data. The resulting estimates can be cross-compared at both local and regional scales. To the best of our knowledge, this is the first large-scale, spatially explicit inventory of slum populations across the Global South countries.

5.1 Robustness of our framework

Figure 6a and 6b illustrate the percentage change in the country-level slum population estimates by comparing the equal weight scenario with two alternative weighting schemes (Section 3.6). We observe that, in both the basic services and UN-Habitat weight scenarios, the variation in slum population estimates for most countries in Africa and South Asia, and Brazil in Latin America remains within ±5%. However, in Southeast Asia and other Latin American countries, the variation ranges from 5% to 10% under the basic service scenario and from -5% to -10% under the UN-Habitat scenario. This suggests that the basic services scenario tends to overestimate slum populations, while the UN-Habitat scenario tends to underestimate them. The three maps of slum population distribution under these three weight scenarios are provided in Figure S4.

It is important to note that countries with changes exceeding ±5% are typically regions where nation-wide household-based surveys are not conducted, which is what our machine learning model is trained to estimate. Overall, our regional models demonstrate strong robustness for countries with available training data, although the weighting scenarios have a relatively large impacts on estimates for countries lacking such data. The equal-weight scenario offers a balanced approach, avoiding the overestimations and underestimations observed in other scenarios.

Figure 6c and 6d compare the performance of regional models with individual country-specific models. To enhance the generalization capabilities of our models, we opt to train regional models rather than individual models for each country. While the regional models show slightly lower performance in terms of RMSE and R^2 compared to single-country models, the differences are minimal and within a comparable range. This indicates that our regional models achieve both high accuracy and strong generalization ability. The full list of individual model performance can be found in Table S5.

https://doi.org/10.5194/essd-2025-260
Preprint. Discussion started: 28 May 2025

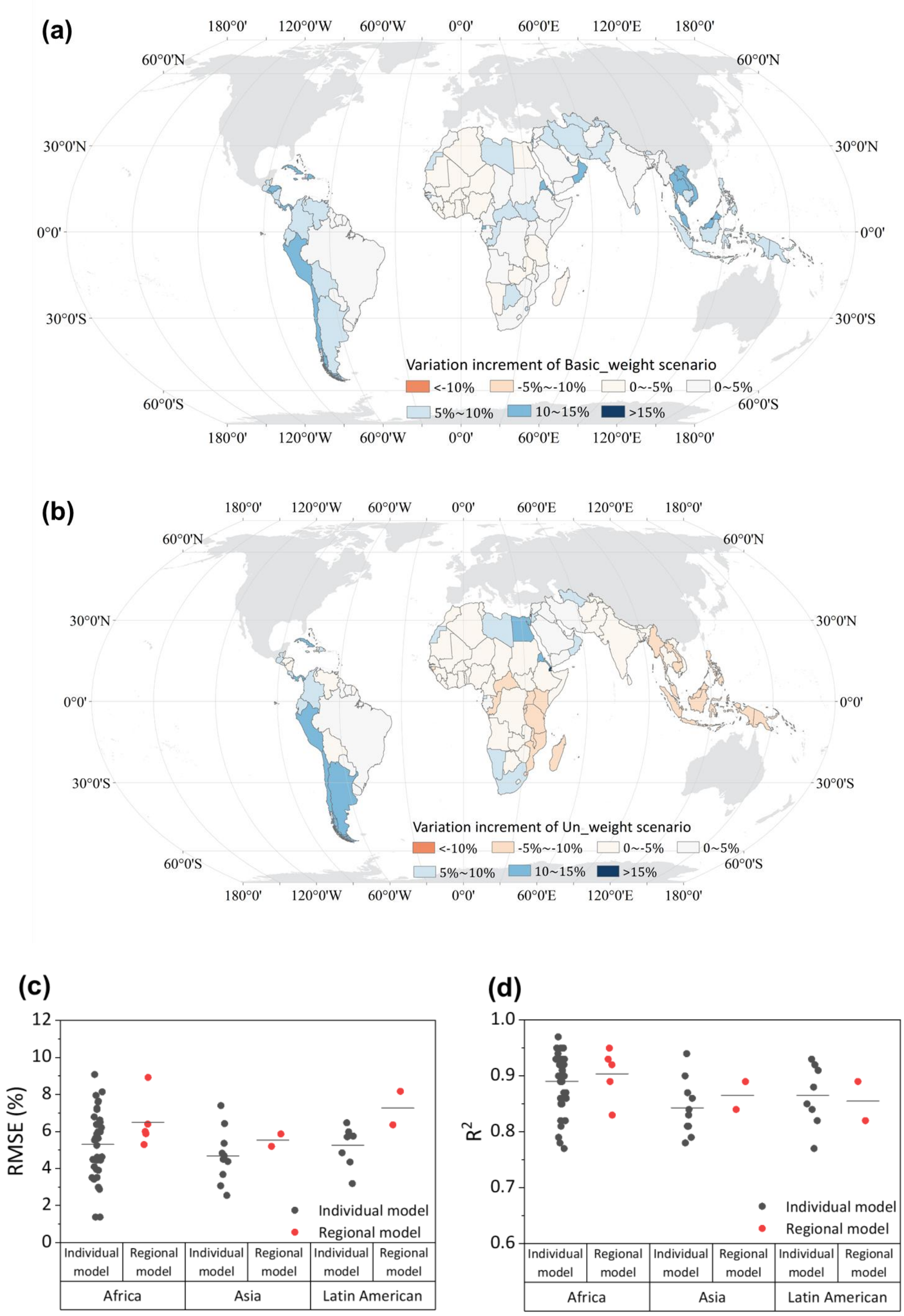

Figure 6 Robustness of the slum population framework and generalization ability of our regional models. Variation in slum population under the basic service (a) and the un-

https://doi.org/10.5194/essd-2025-260
Preprint. Discussion started: 28 May 2025

habitat (b) scenarios. Comparison of RMSE (c) and R^2 (d) performance between regional models and country-specific models

5.2 Spatial resolution and dataset selection

Our maps of slum population distribution and their local shares are presented at spatial resolution of 3.63 arcminutes. This spatial resolution is carefully chosen based on several factors, including the characteristics of satellite imagery, algorithm architecture, and the truth-ground survey data. It is crucial to ensure spatial and temporal match between satellite images and survey data, given the diverse ranges of household-based survey data collected across multiple years and countries. To enhance input data richness, we prefer satellite images with more spectral bands beyond the standard three RGB bands (Wulder et al., 2022), such as Landsat imagery, which offers consistent temporal coverage, global reach, and multiple spectral bands, with a resolution of 30 meters.

The ResNet-34 deep learning architecture used for feature extraction requires the input image to be in a 224x224 pixel format (Wu et al., 2019). Consequently, the resolution of our maps is set at 3.63 arcminutes (6.72 km on equator) to balance these technical requirements. This resolution aligns with other published maps that focus on sub-dimensions of poverty, such as the wealth index and education (Local Burden of Disease Educational Attainment Collaborators, 2020; Yeh et al., 2020), and provides more granular local insights beyond the administrative boundaries typically used in slum population statistics (Tjia and Coetzee, 2022). While our method relies on slum proxy at the cluster level rather than precise slum boundaries, it nonetheless yields valuable insights for large-scale. cross-national estimates of slum populations under current data constraints. Although this resolution does not capture the fine-grained morphology of slums, it effectively identifying populations living in slum-like conditions. Future research can build on this foundation by producing higher-resolution slum data to address this limitation.

The quality of any machine learning or deep learning model relies heavily on the data it is trained on (Meena et al., 2023). The DHS datasets provide accurate and representative household-based survey data on population characteristics and socioeconomic factors. However, a limitation of this dataset is the intentional perturbation of the latitude and longitude coordinates to protect the privacy of the

https://doi.org/10.5194/essd-2025-260
Preprint. Discussion started: 28 May 2025

surveyed households. This perturbation introduces random jitter of 2km in urban areas and 5km in rural areas (Owusu et al., 2021). The 3.63 arcminutes resolution of our maps strikes a balance between preserving privacy, leveraging available data, and ensuring the technological feasibility of our approach.

The grided population dataset is also a critical component for measuring and mapping the slum population. Widely used global population datasets, such as GPWv4.11 (CIESIN et al., 2018), GHS-POP (Pesaresi et al., 2016), World Pop (Stevens et al., 2015), and regional/national products like HRSL (Smith et al., 2019), vary significantly in characteristics and assumptions. These differences arise from the nature and heterogeneity of the input population data, the ancillary data involved, and the methodological framework applied to redistribute population counts to grid cells. Although some regional products like HRSL show commendable accuracy in identifying building footprints and population distributions at finer resolutions, their limited coverage poses challenges for large-scale cross-country comparisons, especially in the Global South.

Considering the 'fitness to use' principle (Juran et al., 1979), the GHS-POP dataset has distinctive advantages closely aligned with our research objectives. Grounded in human settlement information, GHS-POP is effective for spatially refining population data along the urban gradient, making it ideal for our slum population modeling. Additionally, the Global Human Settlement Layer (GHSL), which uses Landsat imagery, aligns with the satellite images used in this study, reducing uncertainties introduced by using different data sources.

5.3 Comparison of results with statistical data

Given the inherent uncertainty in slum population estimates, we cross-validate our mapping results against a broad range of literature data and government statistical data across multiple scales. We first compare our slum population estimates with previous estimates from the literature, which are derived by scaling population counts at individual slum level (Butera et al., 2019; Byuro, 2015; Davis, 2013; Guilmoto and Rajan, 2013; Medeiros et al., 2012; Patel et al., 2019; Sabry, 2009; Taubenböck and Wurm, 2015). Our estimates, indicated by an asterisk (*), fall within the range of these scaled slum population estimates (Figure 7a). Moreover, when compared to city-scale slum population statistics, our results show strong alignment, particularly in Hyderabad and Johannesburg

https://doi.org/10.5194/essd-2025-260
Preprint. Discussion started: 28 May 2025

(Trindade et al., 2021) (Figure 7b). However, for some cities, such as Rio de Janeiro and Dhaka, our results appear to be overestimated. This discrepancy may be because the slum population figures reported in the literature are from around 2014. Factors such as population growth, migration, and slum upgrading projects may have contributed to changes in slum population over time. Additionally, a recent study indicates that relying solely on the spatial extent of morphological slums and grided population datasets can lead to underestimation of the slum population (Breuer et al., 2024). This supports the advantage of our approach.

A comparison of the relative shares of urban slum populations with the World Bank (2018) and UN-Habitat (2021) statistics shows a strong correlation at the national scale ($R^2 > 0.95$) and good agreement at the regional scale (Figure 7c and 7d), with an average RMSE of 14% at the national level.

Several factors likely contribute to the observed discrepancy. First, the definition of slum households in our study does not fully align with those used in the statistical data, which leads to differences in the selection of quantitative indicators. For example, the World Bank's statistics, based on UN-HABITAT definition, adopt a broader perspective that includes housing affordability and security of tenure. Their framework encompasses additional indicators, such as the proportion of households with formal title deeds (to land and housing) and whether a household's monthly net housing expenditure exceeds 30% of their income. Due to data limitations, these specific indicators are not quantified in our study. Instead, we include more detailed sub-indicators, such as access to safely managed drinking water and sanitation services (e.g., households with access to drinking water within a 30-minute round trip), which are absent in the statistical data.

Moreover, the statistical data are compiled from various sources, such as the World Health Surveys (WHS) and Living Standards and Measurement Surveys (LSMS), while our household survey data come from a more singular source. Additionally, in our efforts to generalize a large-scale, unified framework, our regional model estimates for certain countries, especially small island nations, may exhibit bias due to the lack of specific survey data. Further research is needed to refine and validate these results, especially as more high-resolution reference datasets and local-scale models become available in the future.

https://doi.org/10.5194/essd-2025-260
Preprint. Discussion started: 28 May 2025

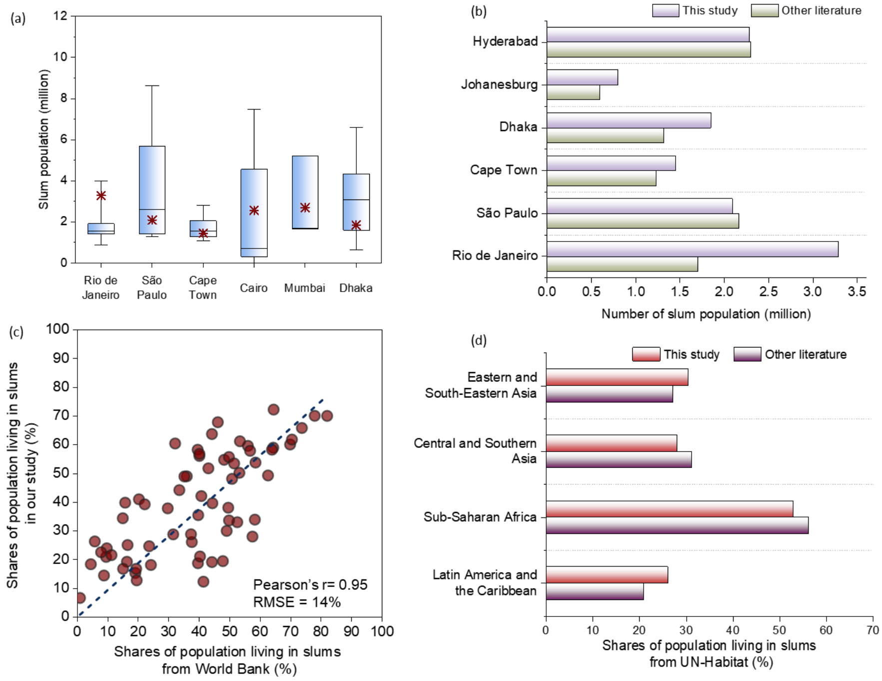

Figure 7 Comparison of our slum population estimates with data from the literature and government statistics, including the absolute numbers and relative shares.

5.4 Implications and future research

Our study provides a foundation for generating large-scale, fine-grained slum population estimates, especially in data-sparse environments across Global South countries. First, this inventory reveals the significant gaps in the efforts of these countries to achieve sustainable development goals. Our estimates provide compelling evidence to raise awareness among governments and organizations about the scale of the slum issue, advocating for more effective allocation of funds and resources to the areas most in need during the slum upgrading projects.

Second, given the overcrowded and unsanitary conditions in slums, which are often associated with waterborne diseases, our maps serve as valuable reference data for addressing environmental issues, health-related challenges, and climate change impacts. Additionally, the data can help policymakers and stakeholders identify slum communities at risk during extreme weather events such as floods

https://doi.org/10.5194/essd-2025-260
Preprint. Discussion started: 28 May 2025

or droughts, supporting the planning and implementation of relocation or emergency response strategies.

Overall, our study has broader implications for urban planning, resource allocation, and the improvement of human well-being among slum populations. The insights provided by our maps support evidence-based decision-making and targeted interventions aimed at achieving sustainable development goals. Since our approach is based on free and openly available data, it can be extended over time to track the dynamics of slum populations at the cluster level. Multi-temporal slum population maps could help uncover the underlying drivers of slum growth, in addition to the forces of local population growth and migration. With more accurate geospatial survey data and higher-resolution satellite imagery, we anticipate significant improvements in the resolution and accuracy of slum population maps. This progress will greatly enhance our understanding of the distribution and scale of slums, enabling more informed decision-making and more effective interventions.

6 Data availability

The maps of slum populations and their local shares in Global South countries are available in the Zalando repository at https://doi.org/10.5281/zenodo.13779003 (Li et al., 2025). All household-based data are available for downloading, free of charge by registered users, from the DHS Program (https://www.dhsprogram.com/data/), satellite images and land cover layers product are download on GEE platform (https://earthengine.google.com/). Global NPP-VIIRS-like nighttime light dataset is from Chen et al. (2020). The Settlement Model grid (GHS-SMOD) and Population Grid (GHS-POP) can be obtained from Global Human Settlement Layer (https://ghsl.jrc.ec.europa.eu/download.php).

7 Conclusions

In this study, we develop a standardized, operational, and bottom-up framework for producing fine-grained, spatially explicit estimates of slum populations. Our framework is based on SDG 11.1 slum household indicators and combines feature extraction techniques with machine learning algorithms. It

https://doi.org/10.5194/essd-2025-260
Preprint. Discussion started: 28 May 2025

integrates household-based surveys, satellite imagery, and grided population data to address the underestimation of slum populations found in prior studies, which often relied heavily on slum geometry. Our approach provides reliable slum population predictions, particularly in data-scarce environments.

The resulting maps are the first comprehensive inventory of slum populations across Global South countries, created with a spatial resolution of 3.63 arcminutes (6.72km at the equator) to protect privacy. The models demonstrate strong performance and robustness, with RMSE values ranging from 5.20% to 10.17% and R^2 values between 0.82 and 0.95. Our estimates fall within the range of scaled slum population estimates from existing literature and exhibit strong correlations with them at both national and regional scales. This approach offers a valuable tool for generating reliable slum population estimates, and the dataset produced will support a wide range of evidence-based decision-making and targeted interventions aimed at achieving city-level sustainable development goals.

Author contributions

D.L. designed the research. D.L. developed the model and datasets. L.S. provided guidance on data validation. L.S and D.L. led the drafting of the manuscript. D.L., L.S. Y.Y. and P.T. contributed significantly to the final writing of the article.

Competing interests

The contact author has declared that none of the authors has any competing interests.

Disclaimer

Publisher's note: Copernicus Publications remains neutral with regard to jurisdictional claims made in the text, published maps, institutional affiliations, or any other geographical representation in this paper.

Acknowledgements

This research was funded by the National Natural Science Foundation of China (72403147), China Postdoctoral Science Foundation (2023M732043), and the Shandong Provincial Natural Science Foundation (ZR2023QG076).

https://doi.org/10.5194/essd-2025-260
Preprint. Discussion started: 28 May 2025

References

Abascal, A., Rothwell, N., Shonowo, A., Thomson, D.R., Elias, P., Elsey, H., Yeboah, G., Kuffer, M. "Domains of deprivation framework" for mapping slums, informal settlements, and other deprived areas in LMICs to improve urban planning and policy: A scoping review. Computers, environment and urban systems 93, 101770, https://doi.org/10.1016/j.compenvurbsys.2022.101770, 2022.

Angeles, G., Lance, P., Barden-O'Fallon, J., Islam, N., Mahbub, A., Nazem, N.I. The 2005 census and mapping of slums in Bangladesh: design, select results and application. International journal of health geographics 8, 1-19, https://doi.org/10.1186/1476-072x-8-32, 2009.

Azzari, G., Lobell, D. Landsat-based classification in the cloud: An opportunity for a paradigm shift in land cover monitoring. Remote Sensing of Environment 202, 64-74, https://doi.org/10.1016/j.rse.2017.05.025, 2017.

Banerjee, A., Banerji, R., Berry, J., Duflo, E., Kannan, H., Mukerji, S., Shotland, M., Walton, M. From proof of concept to scalable policies: Challenges and solutions, with an application. Journal of Economic Perspectives 31, 73-102, https://doi.org/10.1257/jep.31.4.73, 2017.

Baynes, J., Neale, A., Hultgren, T. Improving intelligent dasymetric mapping population density estimates at 30 m resolution for the conterminous United States by excluding uninhabited areas. Earth system science data 14, 2833, https://doi.org/10.5194/essd-14-2833-2022, 2022.

Binzel, C., Fehr, D. Social distance and trust: Experimental evidence from a slum in Cairo. Journal of Development Economics 103, 99-106, https://doi.org/10.1016/j.jdeveco.2013.01.009, 2013.

Björkman, L. Becoming a slum: from municipal colony to illegal settlement in liberalization era Mumbai. Contesting the Indian city: global visions and the politics of the local, 208-240, https://doi.org/10.1002/9781118295823.ch8, 2013.

Breuer, J.H., Friesen, J. Methods to assess spatio-temporal changes of slum populations. Cities 143, 104582, https://doi.org/10.1016/j.cities.2023.104582, 2023.

Breuer, J.H., Friesen, J., Taubenböck, H., Wurm, M., Pelz, P.F. The unseen population: Do we underestimate slum dwellers in cities of the Global South? Habitat International 148, 103056, https://doi.org/10.1016/j.habitatint.2024.103056, 2024.

Buchhorn, M., Smets, B., Bertels, L., De Roo, B., Lesiv, M., Tsendbazar, N.E., Herold, M. and Fritz, S. Copernicus global land service: land cover 100m: collection 3: epoch 2019: Globe, https://zenodo. org/record/3939050, 2020.

Burgert, C.R., Colston, J., Roy, T., Zachary, B. Geographic displacement procedure and georeferenced data release policy for the Demographic and Health Surveys. Icf International, https://doi.org /10.13140/RG.2.1.4887.6563, 2013.

Burke, M., Driscoll, A., Lobell, D.B., Ermon, S. Using satellite imagery to understand and promote sustainable development. Science 371, eabe8628, https://doi.org/10.1126/science.abe8628, 2021.

Butera, F.M., Caputo, P., Adhikari, R.S., Mele, R. Energy access in informal settlements. Results of a wide on site survey in Rio De Janeiro. Energy Policy 134, 110943, https://doi.org/10.1016/j.enpol.2019.110943, 2019.

Byuro, B.P.k.n. Census of slum areas and floating population 2014, http://arks.princeton.edu/ark:/88435/dsp01wm117r42q, 2015.

Chen Z, Yu B, Yang C, Zhou Y, Qian X, Wang C, Wu B, Wu J. An extended time-series (2000–2018) of global NPP-VIIRS-like nighttime light data from a cross-sensor calibration. Earth System Science Data Discussions, 1-34, https://doi.org/10.5194/essd-13-889-2021, 2020.

Chen, T. and Guestrin, C. Xgboost: A scalable tree boosting system, Proceedings of the 22nd acm sigkdd international conference on knowledge discovery and data mining, San Francisco, California, USA, 785–794, https://doi.org/10.1145/2939672.2939785, 2016.

Davis, M. Planet of slums. New Perspectives Quarterly 30, 11-12, https://doi.org/10.1111/npqu.11395, 2013.

Doe, B., Peprah, C., Chidziwisano, J.R. Sustainability of slum upgrading interventions: Perception of low-income households in Malawi and Ghana. Cities 107, 102946, https://doi.org/10.1016/j.cities.2020.102946, 2020.

Elvidge, C.D., Baugh, K., Zhizhin, M., Hsu, F.C., Ghosh, T. VIIRS night-time lights. International journal of remote sensing 38, 5860-5879, https://doi.org/10.1080/01431161.2017.1342050, 2017.

Engin, Z., van Dijk, J., Lan, T., Longley, P.A., Treleaven, P., Batty, M., Penn, A. Data-driven urban management: Mapping the landscape. Journal of Urban Management 9, 140-150, https://doi.org/10.1016/j.jum.2019.12.001, 2020.

Ezeh, A., Oyebode, O., Satterthwaite, D., Chen, Y.-F., Ndugwa, R., Sartori, J., Mberu, B., Melendez-Torres, G.J., Haregu, T., Watson, S.I. The history, geography, and sociology of slums and the health problems of people who live in slums. The lancet 389, 547-558, https://doi.org/10.1016/s0140-6736(16)31650-6, 2017.

Fu, B., Wang, S., Zhang, J., Hou, Z., Li, J. Unravelling the complexity in achieving the 17 sustainable-development goals. National Science Review 6, 386-388, https://doi.org/10.1093/nsr/nwz038, 2019.

Gram-Hansen, B.J., Helber, P., Varatharajan, I., Azam, F., Coca-Castro, A., Kopackova, V., Bilinski, P. Mapping informal settlements in developing countries using machine learning and low resolution multi-spectral data, Proceedings of the 2019 AAAI/ACM Conference on AI, Ethics, and Society, pp. 361-368, https://doi.org/10.1145/3306618.3314253, 2019.

Guan, X., Wei, H., Lu, S., Dai, Q., Su, H. Assessment on the urbanization strategy in China: Achievements, challenges and reflections. Habitat International 71, 97-109, https://doi.org/10.1016/j.habitatint.2017.11.009, 2018.

Guilmoto, C.Z., Rajan, S.I. Fertility at the district level in India: Lessons from the 2011 census. Economic and Political weekly, 59-70, http://www.ceped.org/wp, 2013.

Haberl H, Wiedenhofer D, Schug F, Frantz D, Virág D, Plutzar C, Gruhler K, Lederer J, Schiller G, Fishman T, Lanau M. High-resolution maps of material stocks in buildings and infrastructures in Austria and Germany. Environmental science & technology 55(5): 3368-79, https://doi.org/10.1021/acs.est.0c05642, 2021.

Hardoy, J.E., Mitlin, D., Satterthwaite, D. Environmental problems in an urbanizing world: finding solutions in cities in Africa, Asia and Latin America. Routledge, https://doi.org/10.4324/9781315071732, 2013.

He, K., Zhang, X., Ren, S., Sun, J. Deep residual learning for image recognition, Proceedings of the IEEE conference on computer vision and pattern recognition, pp. 770-778, https://doi.org/10.1109/cvpr.2016.90, 2016.

Hohmann, J. The right to housing: Law, concepts, possibilities. Bloomsbury Publishing, https://doi.org/10.5040/9781472566416, 2013.

https://doi.org/10.5194/essd-2025-260
Preprint. Discussion started: 28 May 2025

Hsu, F.-C., Baugh, K.E., Ghosh, T., Zhizhin, M., Elvidge, C.D. DMSP-OLS radiance calibrated nighttime lights time series with intercalibration. Remote Sensing 7, 1855-1876, https://doi.org/10.3390/rs70201855, 2015.

Ibrahim, M.R., Titheridge, H., Cheng, T., Haworth, J. predictSLUMS: A new model for identifying and predicting informal settlements and slums in cities from street intersections using machine learning. Computers, Environment and Urban Systems 76, 31-56, https://doi.org/10.1016/j.compenvurbsys.2019.03.005, 2019.

Juran, J.M., Gryna, F.M., Bingham, R.S. (1979) Quality control handbook. McGraw-Hill New York.

Li, D., Sun, L., Yu, Y., Tian, P. Geospatial micro-estimates of slum populations in 129 Global South countries using machine learning and public data. Available at https://doi.org/10.5281/zenodo.13779003, 2025.

Kingma, D.P., Ba, J. Adam: A method for stochastic optimization. arXiv preprint arXiv:1412.6980, https://doi.org/10.48550/arXiv.1412.6980, 2014.

Local Burden of Disease Educational Attainment Collaborators. Mapping disparities in education across low-and middle-income countries. Nature 577, 235-238, https://doi.org/10.1038/s41586-019-1872-1, 2020.

Mahabir, R., Agouris, P., Stefanidis, A., Croitoru, A., Crooks, A.T. Detecting and mapping slums using open data: A case study in Kenya. International Journal of Digital Earth 13, 683-707, https://doi.org/10.1080/17538947.2018.1554010, 2020.

Marx, B., Stoker, T., Suri, T. The economics of slums in the developing world. Journal of Economic perspectives, *27*(4), 187-210, https://doi.org/10.1257/jep.27.4.187, 2013.

Medeiros, S.d.S., Pinto, T.F., Hernan Salcedo, I., Cavalcante, A.d.M.B., Perez Marin, A.M., Tinôco, L.B.d.M. Sinopse do censo demográfico para o semiárido brasileiro. Instituto Nacional de Seminário (INSA)., http://livroaberto.ibict.br/handle/1/941, 2012.

Meena, S., Nava, L., Bhuyan, K., Puliero, S., Soares, L., Dias, H., Floris, M., Catani, F. HR-GLDD: a globally distributed dataset using generalized deep learning (DL) for rapid landslide mapping on high-resolution (HR) satellite imagery. Earth Syst. Sci. Data 15, 3283–3298, https://doi.org/10.5194/essd-15-3283-2023, 2023.

Moreno, E.L. Slums of the world: The face of urban poverty in the new millennium?: Monitoring the millennium development goal, target 11--world-wide slum dweller estimation. Un-Habitat, https://digitallibrary.un.org/record/515731, 2003.

Mwaniki, D., Ndugwa, R. The Global Urban Monitoring Approach Taken by UN-HABITAT. Stadtentwicklung beobachten, messen und umsetzen. Informationen zur Raumentwicklung (IzR), 32-43, https://biblioscout.net/article/99.140005/izr202101003201, 2021.

Nowak, M. Introduction to the international human rights regime. Brill, https://doi.org/10.1163/9789004479074, 2003.

Oppenheimer, M., Campos, M., Warren, R., Birkmann, J., Luber, G., O'Neill, B., Takahashi, K., Brklacich, M., Semenov, S., Licker, R. Emergent risks and key vulnerabilities, Climate change 2014 impacts, adaptation and vulnerability: part a: global and sectoral aspects. Cambridge University Press, pp. 1039-1100, https://doi. org/10.1017/CBO9781107415379, 2015.

Owusu, M., Kuffer, M., Belgiu, M., Grippa, T., Lennert, M., Georganos, S., Vanhuysse, S. (2021) Towards user-driven earth observation-based slum mapping. Computers, environment and urban systems 89, 101681, https://doi.org/10.1016/j.compenvurbsys.2021.101681, 2021.

Pan, S.J., Yang, Q. A survey on transfer learning. IEEE Transactions on knowledge and data

https://doi.org/10.5194/essd-2025-260
Preprint. Discussion started: 28 May 2025

engineering 22(10):1345-59, https://doi.org/10.1109/TKDE.2009.191, 2009.

Parikh, P., Parikh, H., McRobie, A. The role of infrastructure in improving human settlements. Proceedings of the Institution of Civil Engineers-Urban Design and Planning 166, 101-118, https://doi.org/10.1680/udap.10.00038, 2013.

Patel, A., Joseph, G., Shrestha, A., Foint, Y. (2019) Measuring deprivations in the slums of Bangladesh: implications for achieving sustainable development goals. Housing and Society 46, 81-109.

Pedro, A.A., Queiroz, A.P. (2019) Slum: Comparing municipal and census basemaps. Habitat International 83, 30-40, https://doi.org/10.1596/32084, 2019.

Persello, C., Kuffer, M. Towards uncovering socio-economic inequalities using VHR satellite images and deep learning, IGARSS 2020-2020 IEEE International Geoscience and Remote Sensing Symposium. IEEE, pp. 3747-3750, https://doi.org/10.1109/igarss39084.2020.9324399, 2020.

Pesaresi, M., Ehrlich, D., Ferri, S., Florczyk, A.J., Freire, S., Halkia, M., Julea, A., Kemper, T., Soille, P., Syrris, V. Operating procedure for the production of the Global Human Settlement Layer from Landsat data of the epochs 1975, 1990, 2000, and 2014. Publications Office of the European Union Luxembourg, https://doi.org/10.2788/253582, 2016.

Rentschler, J., Avner, P., Marconcini, M., Su, R., Strano, E., Vousdoukas, M., Hallegatte, S. Global evidence of rapid urban growth in flood zones since 1985. Nature 622, 87-92, https://doi.org/10.1038/s41586-023-06468-9, 2023.

Robinson, C., Hohman, F., Dilkina, B. A deep learning approach for population estimation from satellite imagery, Proceedings of the 1st ACM SIGSPATIAL Workshop on Geospatial Humanities, pp. 47-54, https://doi.org/10.1145/3149858.3149863, 2017.

Rogler, L.H. Slum Neighborhoods in Latin America. Journal of Inter-American Studies 9, 507-528, https://doi.org/10.2307/164857, 1967.

Roy, D.P., Kovalskyy, V., Zhang, H.K., Vermote, E.F., Yan, L., Kumar, S.S. and Egorov, A. Characterization of Landsat-7 to Landsat-8 reflective wavelength and normalized difference vegetation index continuity. Remote sensing of Environment 185, 57-70, https://doi.org/10.1016/j.rse.2015.12.024, 2016.

Russakovsky, O., Deng, J., Su, H., Krause, J., Satheesh, S., Ma, S., Huang, Z., Karpathy, A., Khosla, A., Bernstein, M. Imagenet large scale visual recognition challenge. International journal of computer vision 115, 211-252, https://doi.org/10.1007/s11263-015-0816-y, 2015.

Rutstein, S.O., Staveteig, S. Making the demographic and health surveys wealth index comparable. ICF international Rockville, MD, https://www.dhsprogram.com/pubs/pdf/MR9/MR9.pdf, 2014.

Sabry, S. Poverty lines in Greater Cairo: underestimating and misrepresenting poverty. IIED, https://www.iied.org/10572iied, 2009.

Satterthwaite, D., Archer, D., Colenbrander, S., Dodman, D., Hardoy, J., Mitlin, D., Patel, S. Building resilience to climate change in informal settlements. One Earth 2, 143-156, https://doi.org/10.1016/j.oneear.2020.02.002, 2020.

Schetke, S., Haase, D., Kötter, T. Towards sustainable settlement growth: A new multi-criteria assessment for implementing environmental targets into strategic urban planning. Environmental Impact Assessment Review 32, 195-210, https://doi.org/10.1016/j.eiar.2011.08.008, 2012.

Schiavina, M., Melchiorri, M., Pesaresi, M., Politis, P., Carneiro Freire, S., Maffenini, L., Florio, P.,

https://doi.org/10.5194/essd-2025-260
Preprint. Discussion started: 28 May 2025

Open Access Earth System Science Data Discussions

Ehrlich, D., Goch, K., Tommasi, P. GHSL data package 2022: Public release GHS P2022. KJ-07–22–357-EN-N (online), KJ-07–22–357-EN-C (print), https://doi.org/10.2760/19817, 2022.

Shi, Q., Liu, M., Marinoni, A., Liu, X. UGS-1m: Fine-grained urban green space mapping of 34 major cities in China based on the deep learning framework. Earth System Science Data Discussions 15, 555-577, https://doi.org/10.5194/essd-15-555-2023, 2023.

Sietchiping, R., Yoon, H. J. What drives slum persistence and growth? Empirical evidence from sub-Saharan Africa. International Journal of Advances Studies and Research in Africa 1, 1-22, http://www.africascience.org, 2010.

Singh, B.N. Socio-economic conditions of slums dwellers: a theoretical study. Kaav International Journal of Arts, Humanities & Social Sciences 3, 5-20, https://www.kaavpublications.org/abstract/article-236.pdf, 2016.

Smith, A., Bates, P.D., Wing, O., Sampson, C., Quinn, N., Neal, J. New estimates of flood exposure in developing countries using high-resolution population data. Nature communications 10, 1814, https://doi.org/10.1038/s41467-019-09282-y, 2019.

Stevens, F.R., Gaughan, A.E., Linard, C., Tatem, A.J. Disaggregating census data for population mapping using random forests with remotely-sensed and ancillary data. PloS one 10, e0107042, https://doi.org/10.1371/journal.pone.0107042, 2015.

Tamiminia, H., Salehi, B., Mahdianpari, M., Quackenbush, L., Adeli, S., Brisco, B. Google Earth Engine for geo-big data applications: A meta-analysis and systematic review. ISPRS journal of photogrammetry and remote sensing 164, 152-170, https://doi.org/10.1016/j.isprsjprs.2020.04.001, 2020.

Taubenböck, H., Wurm, M. Globale Urbanisierung–Markenzeichen des 21. Jahrhunderts. Globale Urbanisierung: Perspektive aus dem All, 5-10, https://doi.org/10.1007/978-3-662-44841-0_2, 2015.

Tellman, B., Sullivan, J.A., Kuhn, C., Kettner, A.J., Doyle, C.S., Brakenridge, G.R., Erickson, T.A., Slayback, D.A. Satellite imaging reveals increased proportion of population exposed to floods. Nature 596, 80-86, https://doi.org/10.1038/s41586-021-03695-w, 2021.

Thomson, D.R., Kuffer, M., Boo, G., Hati, B., Grippa, T., Elsey, H., Linard, C., Mahabir, R., Kyobutungi, C., Maviti, J. Need for an integrated deprived area "slum" mapping system (IDEAMAPS) in low- and middle-income countries (LMICs). Social Sciences 9, 80, https://doi.org/10.3390/socsci9050080, 2020.

Thomson, D.R., Linard, C., Vanhuysse, S., Steele, J.E., Shimoni, M., Siri, J., Caiaffa, W.T., Rosenberg, M., Wolff, E., Grippa, T. Extending data for urban health decision-making: a menu of new and potential neighborhood-level health determinants datasets in LMICs. Journal of urban health 96, 514-536, https://doi.org/10.1007/s11524-019-00363-3, 2019.

Thomson, D.R., Stevens, F.R., Chen, R., Yetman, G., Sorichetta, A., Gaughan, A.E. Improving the accuracy of gridded population estimates in cities and slums to monitor SDG 11: Evidence from a simulation study in Namibia. Land Use Policy 123, 106392, https://doi.org/10.1016/j.landusepol.2022.106392, 2022.

Tian, P., Zhong, H., Chen, X., Feng, K., Sun, L., Zhang, N., Shao, X., Liu, Y. and Hubacek, K. Keeping the global consumption within the planetary boundaries. Nature, 635, 625-630, https://doi.org/10.1038/s41586-024-08154-w, 2024.

Tjia, D., Coetzee, S. Geospatial information needs for informal settlement upgrading–A review. Habitat International 122, 102531, https://doi.org/10.1016/j.habitatint.2022.102531, 2022.

https://doi.org/10.5194/essd-2025-260
Preprint. Discussion started: 28 May 2025

Trindade, T.C., MacLean, H.L., Posen, I.D. Slum infrastructure: Quantitative measures and scenarios for universal access to basic services in 2030. Cities 110, 103050, https://doi.org/10.1016/j.cities.2020.103050, 2021.

UN-Habitat. The challenge of slums: global report on human settlements 2003. Management of Environmental Quality: An International Journal 15, 337-338, https://doi.org/10.1108/meq.2004.15.3.337.3, 2004.

UN-Habitat. World Cities Report 2020: The Value of Sustainable Urbanization. https://unhabitat.org/world-cities-report-2020-the-value-of-sustainable-urbanization, 2020.

UN-habitat. Urban indicators database. https://data.unhabitat.org/pages/housing-slums-and-informal-settlements, 2021.

Center for International Earth Science Information Network (CIESIN), Columbia University. Gridded Population of the World, Version 4 (GPWv4): Population Density, Revision 11. NASA SEDAC. https://doi.org/10.7927/H4F47M65, 2018.

Weber, H. Politics of 'leaving no one behind': contesting the 2030 Sustainable Development Goals agenda, The Politics of Destination in the 2030 Sustainable Development Goals. Routledge, pp. 64-79, https://doi.org/10.4324/9780429490507-4, 2018.

Wisner, B. Vulnerability as concept, model, metric, and tool, Oxford research encyclopedia of natural hazard science, https://doi.org/10.1093/acrefore/9780199389407.013.25, 2016.

World Bank Group. Population living in slums (% of urban population). https://data.worldbank.org/indicator/EN.POP.SLUM.UR.ZS, 2018.

Wu, Z., Shen, C., Van Den Hengel, A. Wider or deeper: Revisiting the resnet model for visual recognition. Pattern recognition 90, 119-133, https://doi.org/10.1016/j.patcog.2019.01.006, 2019.

Wulder, M.A., Roy, D.P., Radeloff, V.C., Loveland, T.R., Anderson, M.C., Johnson, D.M., Healey, S., Zhu, Z., Scambos, T.A., Pahlevan, N. Fifty years of Landsat science and impacts. Remote Sensing of Environment 280, 113195, https://doi.org/10.1016/j.rse.2022.113195, 2022.

Wurm, M., Stark, T., Zhu, X.X., Weigand, M., Taubenböck, H. Semantic segmentation of slums in satellite images using transfer learning on fully convolutional neural networks. ISPRS journal of photogrammetry and remote sensing 150, 59-69, https://doi.org/10.1016/j.isprsjprs.2019.02.006, 2019.

Wurm, M., Taubenböck, H., Weigand, M., Schmitt, A. Slum mapping in polarimetric SAR data using spatial features. Remote sensing of environment 194, 190-204, https://doi.org/10.1016/j.rse.2017.03.030, 2017.

Yeh, C., Perez, A., Driscoll, A., Azzari, G., Tang, Z., Lobell, D., Ermon, S., Burke, M. Using publicly available satellite imagery and deep learning to understand economic well-being in Africa. Nature communications 11, 2583, https://doi.org/10.1038/s41467-020-16185-w, 2020.

Zhou, Y., Li, X., Chen, W., Meng, L., Wu, Q., Gong, P., Seto, K.C. Satellite mapping of urban built-up heights reveals extreme infrastructure gaps and inequalities in the Global South. Proceedings of the National Academy of Sciences 119, e2214813119, https://doi.org/10.1073/pnas.2214813119, 2022.